Eur. Phys. J. D **1**, 79–84 (1998)

THE EUROPEAN PHYSICAL JOURNAL D

Diagnostics of mixed van der Waals clusters

E. Fort[a], F. Pradère, A. De Martino, H. Vach, and M. Châtelet

Laboratoire d'Optique Quantique du CNRS, Ecole Polytechnique, 91128 Palaiseau Cedex, France

Received: 6 October 1997 / Revised: 4 November 1997 / Accepted: 13 November 1997

Abstract. We present two complementary techniques that provide detailed diagnostics of supersonic beams involving several species. First, surface scattering, together with quadrupole mass spectrometer detection, yields the monomer percentage for each species within the beam. Second, analyses of beam profiles for different masses after scattering by a buffer gas permit determination of mixed cluster presence and, if any, of cluster sizes and compositions. The two techniques are applied to supersonic expansions of an argon-nitrogen mixture. We discuss the results that provide new insight in binary nucleation processes.

PACS. 36.40.-c Atomic and molecular clusters

1 Introduction

Atomic and molecular van der Waals clusters have been the object of extensive experimental and theoretical studies. Recently, new developments involving mixed molecular beams and clusters have provided a unique way for catalysis studies and cluster investigations [1–8]. Such mixed clusters can be produced essentially by two techniques:

- in the first one, previously prepared pure clusters "pick-up" atoms or molecules of another species from a buffer gas or from a crossed beam [3]. This technique allows generation of mixed clusters with a large variety of compositions, but increases beam divergence and speed dispersion;
- the second technique consists in the expansion of a gas mixture with two or more components which then nucleates into clusters, forming mixed beams with low angular and speed dispersions. However, the involved nucleation process is quite complicated and not fully understood and the final characteristics of the beam cannot be easily predicted from the initial gas mixture.

The analysis of such molecular beams raises some intriguing questions: are there any clusters in the beam? If any, are they pure or mixed? What about their compositions and average sizes? Are there any monomers left in the beam?

In this paper, we investigate these issues by two complementary techniques.

Together, they open new prospects for nucleation studies. The first one uses a surface scattering process [9] to provide the percentage of monomers, *i.e.* uncondensed matter, of each species present in the beam. The second relies on analysis of beam profiles after scattering by a buffer gas. It proves the possible existence of hetero-clusters and, if any, their composition and average sizes. We apply these methods to a nitrogen-argon beam obtained by expansion of a gas mixture and comment the results.

[a] e-mail: `fort@leonardo.polytechnique.fr`

2 Experimental

2.1 The apparatus

The basic part of the experimental apparatus has been described previously [10]. We present, in the following, the main features relevant for this paper.

The gas mixture is prepared by compressing pure gases in a bottle. Its composition is controlled by a weighting technique. For the measurements presented here, we use either pure argon or pure nitrogen or a gas mixture composed of 0.91 ± 0.01 molar fraction (mf) nitrogen and 0.09 ± 0.01 mf argon.

The gas, at room temperature, expands in a supersonic Campargue type beam generator through a sonic nozzle of 0.25 mm diameter. The stagnation pressure can be varied from 0.1 to 50 bars leading to average sizes of van der Waals clusters up to one thousand monomers for pure nitrogen and up to ten thousand monomers for pure argon. The beam passes through three differentially pumped chambers before entering an Ultra-High Vacuum (UHV) chamber. We can introduce a pressure controlled buffer gas in the third chamber either directly to permit average size determination [11] or through a small pipe in the beam path for pick-up processes [12]. Beam diagnostics are performed using a rotatable Quadrupole Mass Spectrometer (QMS) in the UHV chamber. To allow lock-in detection and time-of-flight measurements, the beam is chopped before entering this chamber. The QMS mass range extends to 200 amu. It consequently detects only monomers and quite small van der Waals complexes (dimers and trimers)

of the species under consideration. The finally detected particles are either initially present in the beam or are produced by fragmentation of the incident large clusters inside the ionization head. Besides, the QMS rotates around the center of the UHV chamber where a surface sample can be placed to intercept the beam. Hence, the QMS can be used to detect particles directly within the beam or scattered by the surface, giving the density and time-of-flight distributions.

The surface is a Highly Oriented Pyrolytic Graphite (HOPG) sample at a temperature of $T_S = 440$ K. The incidence angle (measured from the surface normal) used for the presented results is $\theta_{inc} = 20°$.

2.2 The surface scattering process

As we have previously demonstrated for large argon clusters scattered off a graphite surface [9], large van der Waals cluster scattering is physically understood by a Leidenfrost process in which the normal part of the incoming cluster kinetic energy is converted into thermal energy while the tangential part is nearly entirely preserved.

The scattering lobes and time-of-flight distributions for a beam of pure clusters present three different components. They have been assigned respectively to three different channels:

a) a thermal evaporation component of monomers due to the heating of the parent cluster gliding along the surface. This channel is well modelized by a thermokinetic model [13];
b) a grazing component due to a cluster surviving the collision in the case when the normal kinetic energy is not sufficient to evaporate the entire incident cluster; it has been modelized by the dynamic zone structure model [14];
c) a diffuse component resulting from atoms getting trapped and desorbing after a certain residence time. This channel has been modelized by the Lambert cosine law [15].

Under our present experimental conditions ($\theta_{inc} = 20°$), the grazing component does not appear and the angular distributions are well modelized with only two components: the Evaporation Component (EC) and the Diffuse Component (DC).

2.3 Determination of monomer percentages in the beam

Monomers and clusters initially present in the incident beam give different scattering signatures after collision with the surface as shown in Figure 1. This figure presents the scattering lobes measured at argon monomer mass setting for argon-nitrogen mixed beams with stagnation pressures of 1, 11 and 21 bars, respectively.

At the lowest stagnation pressure, the beam is only composed of monomers. The shape of this lobe does not change when varying the stagnation pressure as long as the condensation process does not start in the expansion. Therefore, we use the experimental results given by Figure 1a to define the shape of the Monomer Signature (MS).

The other experimental curves given in Figures 1b and 1c are fitted by taking into account the monomer signature and the cluster scattering signature described by the models mentioned above [13–15]. These models, which have also been verified for pure nitrogen clusters [16], have been tentatively extended for each species of mixed argon-nitrogen clusters. In the general case of a beam composed of monomers flying together with mixed clusters, these models permit to fit the experimental lobes as function of scattering angle θ_s obtained for each species X with a linear combination of three components:

$$\alpha(\mathrm{X})\mathrm{EC}(\mathrm{X},\theta_s) + \beta(\mathrm{X})\mathrm{DC}(\mathrm{X},\theta_s) + \gamma(\mathrm{X})\mathrm{MS}(\mathrm{X},\theta_s). \quad (1)$$

The Figure 1c shows typical experimental results obtained for "high" stagnation pressures for which there is only a small amount of monomers left in the incident beam, *i.e.* $\gamma(\mathrm{Ar})$ tends to zero. The Figure 1b illustrates an intermediate situation in which the three components appear. The experimental data are well fitted by our model.

The percentage of monomers in the beam $\rho_X(Pr)$ of each species X for the stagnation pressure Pr is evaluated from the following formula:

$$\rho_X(Pr) = \frac{(\gamma(\mathrm{X})/\Phi(\mathrm{X}))_{Pr}}{(\gamma(\mathrm{X})/\Phi(\mathrm{X}))_{Pr_0}} \quad (2)$$

where $\Phi(\mathrm{X})$ is the mass flux in the beam for the species X and Pr_0 corresponds to a low stagnation pressure for which X particles do not condensate, *i.e.* $\rho_X(Pr_0) = 100\%$ (*cf.* Fig. 1a). $\Phi(\mathrm{X})$ is proportional to the QMS signal at the top of the beam profile. Indeed, this profile does not change with stagnation pressure as it is limited by a diaphragm placed inside the UHV chamber.

2.4 Existence and characterization of mixed clusters

The existence and the characterization of mixed clusters relies on the analysis of beam profiles for different mass settings of the QMS with or without a buffer gas. To perform these experiments, we temporarily remove the diaphragm mentioned above.

Figure 2 shows typical results without buffer gas of normalized beam profiles for argon monomers, nitrogen monomers, and mixed dimer (ArN_2) mass settings for the nitrogen-argon gas mixture at a high stagnation pressure.

The normalized beam profiles measured for each of the two species, Ar and N_2, correspond exactly. In addition, the normalized profile for mixed ArN_2 dimer mass setting is quite identical. As it is unlikely to produce mixed dimers by monomer- monomer collisions directly inside the QMS head for the very low pressures existing in the detector, these mixed dimers have survived the QMS fragmentation. Consequently, they could be either initially present in the incoming beam or issued from fragmentation of large mixed clusters. The broadening of the beam profiles by a buffer gas will give the origin of those detected dimers.

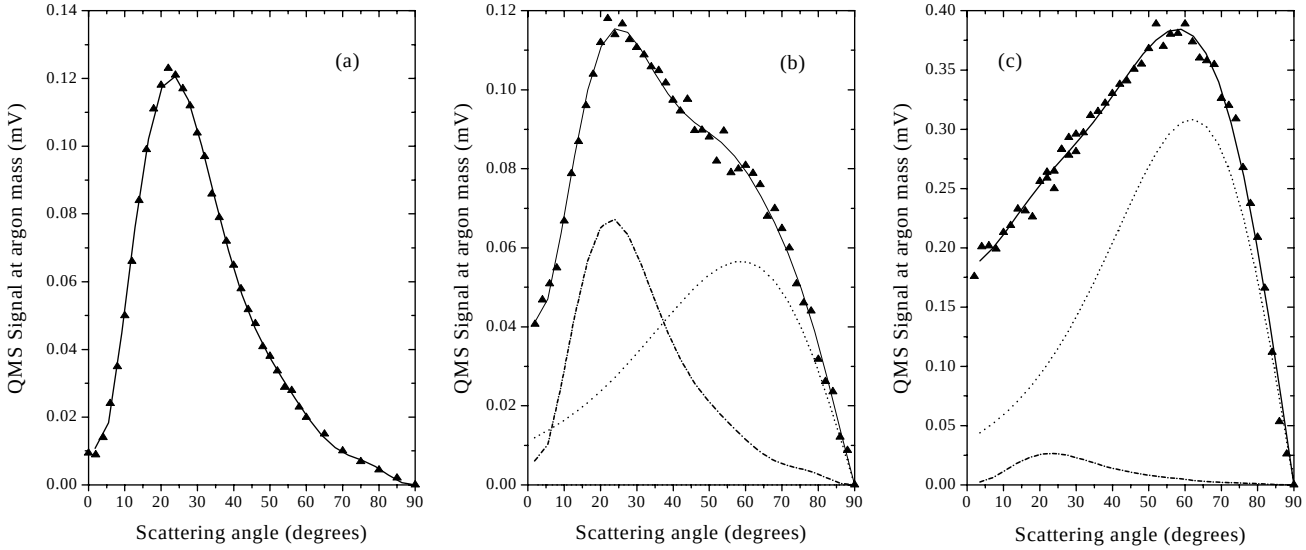

Fig. 1. Typical angular distributions of a nitrogen-argon gas mixture beam scattered off the HOPG surface measured at argon monomers mass setting for different stagnation pressures: (a) 1 bar, signature of incident monomers, (b) 11 bars, beam composed of monomers and clusters and (c) 21 bars, beam essentially composed of clusters. Triangles: experimental data, full line: total fit, dashed line: monomer component and dotted line: evaporation channel component (see text).

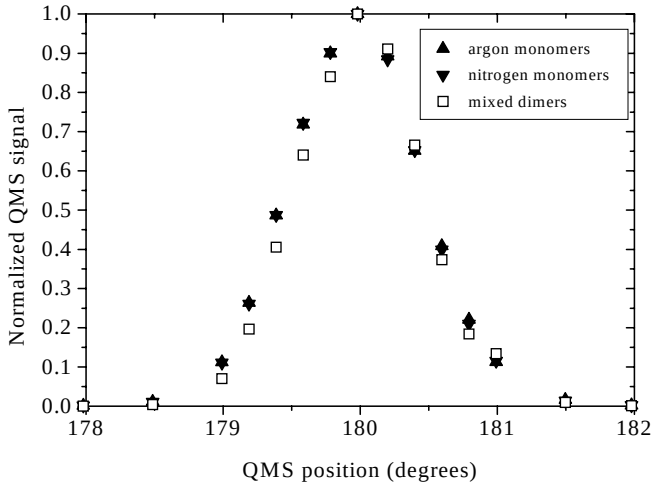

Fig. 2. Normalized beam profiles for an argon-nitrogen mixture obtained with the QMS tuned respectively to argon monomer, nitrogen monomer and mixed dimer masses. The stagnation pressure is 46 bars.

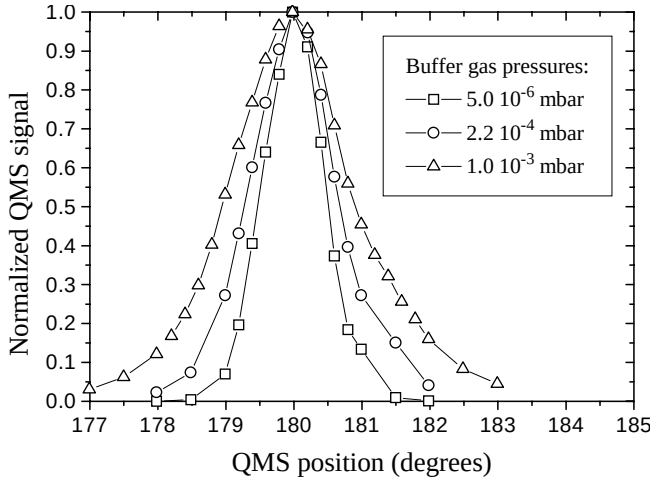

Fig. 3. Broadening of mixed ArN_2 dimer profiles for different buffer gas pressures for a 0.91 mf nitrogen—0.09 mf argon mixed gas composition.

Figure 3 shows buffer gas broadening of the beam profiles for ArN_2 dimer mass setting for the nitrogen-argon mixture beam. As small particles (dimers, trimers, ...) initially present in an incident beam are highly deviated during collisions with buffer gas atoms [11], the very presence of these broadened profiles proves that the detected ArN_2 mixed dimers are issued from larger mixed clusters. For clarity, we do not add in Figure 3 the measured broadened profiles for Ar and N_2 mass settings. For a given buffer gas pressure, these two profiles correspond exactly to the one of mixed ArN_2 dimers. This behavior confirms that all the detected particles are issued from the QMS fragmentation of the same large $Ar_m(N_2)_n$ mixed cluster.

Angular distribution broadening of the beams caused by passing through a buffer gas as shown in Figure 3, has been used to determine average sizes for pure clusters. The shape and width of the beam profile after scattering by the buffer gas are evaluated theoretically as functions of buffer gas pressure and atom-cluster collision cross-section. This technique is valid only for stagnation pressures high enough so that the uncondensed particle proportion in the beam is sufficiently low as can be verified by the surface scattering technique.

To extend the profile broadening technique to mixed cluster size measurements it is necessary to know the composition of these clusters to evaluate the cluster cross-sections and masses. The beam composition is deduced

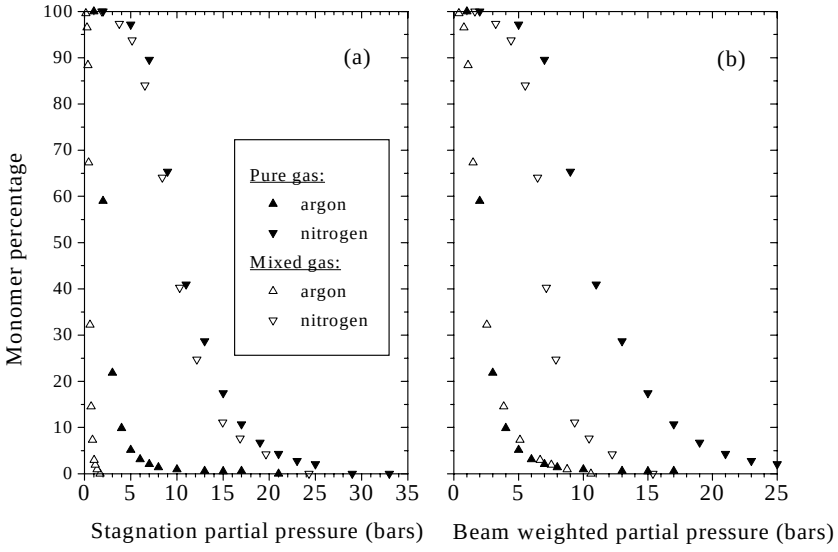

Fig. 4. Argon and nitrogen monomer percentages in the beam for pure argon, pure nitrogen and a 0.91 mf nitrogen—0.09 mf argon gas mixture plotted against (a) stagnation partial pressures and (b) total stagnation pressure weighted by the mf of each species in the beams.

from the signal intensities of the profiles given by the QMS which has been tuned to each of the monomer masses and corrected by the detector sensitivity. Using the surface scattering technique it is possible to take into account the uncondensed matter (residual monomers) and, thus, to deduce the cluster composition.

In the case of mixed argon-nitrogen clusters, their compositions are needed only for mass determination. Indeed, the two species having about the same crystal lattice spacing, the cluster cross-sections only depend on the number of atoms they contain.

3 Results and discussions

The nitrogen molar fraction in the mixture is about 10 times larger than the argon mf before expansion and the particle speed in the beam has been measured to be the same as that with pure nitrogen (about 750 m/s). In a first step, nitrogen can be viewed as the carrier gas and argon as the seeded gas during the expansion process.

The percentages of monomers obtained with the surface scattering technique for the argon-nitrogen gas mixture are presented in Figure 4a together with pure gas results for each species as functions of partial stagnation pressures (obtained from the initial gas molar fraction before expansion).

Figure 4a seems to show that argon does not significantly help nitrogen to nucleate as N_2 monomer percentages inside the argon-nitrogen beam and inside a pure nitrogen beam are nearly identical for different stagnation pressures.

This is quite unexpected. Indeed, if we look at the binding energies we find that the argon-argon binding energy is higher than the nitrogen-nitrogen one and about the same as the argon-nitrogen one (120 K, 95 K [17] and 121 K [18], respectively). Consequently, we would expect that argon atoms act like seeds, enhancing nitrogen nucleation. Besides, because of the presence of argon, we might also expect mixed- dimer formation which is a new way to reduce the nitrogen monomer percentage as compared with pure nitrogen expansion. Moreover, due to its higher heat capacity ratio (gamma) than nitrogen, argon tends to increase the cooling effect of the expansion compared with a pure nitrogen gas, thus favoring nitrogen nucleation [19].

On the contrary, Figure 4a seems to indicate that the nitrogen presence helps argon to nucleate as argon monomers remaining in the argon-nitrogen beam desappear faster than in the pure argon beam with increasing pressure. This is again unexpected because of the same type of arguments as presented before (reduction of the cooling effect due to the low gamma of nitrogen and binding energy considerations). Moreover, changing from argon to nitrogen as the third particle X in the reaction $Ar + Ar + X \leftrightarrow Ar_2 + X^*$ does not displace the balance towards dimer formation during expansion. Experimental results prove that nitrogen is indifferent to the argon dimer formation reaction [20].

The argon molar fractions have been deduced from the measurement of argon and nitrogen QMS signal intensities in the beam. Morover, since the percentages of remaining monomers for each species in the beam versus the total stagnation pressure have been determined, this yields to the average argon molar fraction in the mixed clusters contained in the beam. Results are shown in Figure 5.

It appears that the argon concentration becomes higher in the beam than before the expansion (14% to 35% in regard to the 10% before expansion). The heavier particles (argon) tend to be focused upstream from the skimmer entrance (Mach-number focusing effect) [21]. A maximum of 0.35 for argon mf is reached at 13 bars before the argon mf decreases slowly for higher stagnation pressures. We think that this, again, is essentially the result of a balance between the Mach-number focusing effect and the rates of nucleation.

Considering now the cluster composition given in Figure 5, at a stagnation pressure of 5 bars, the mf of argon in the clusters is about 0.24. It is higher than the mf of argon in the beam (0.14) since argon tends to nucleate

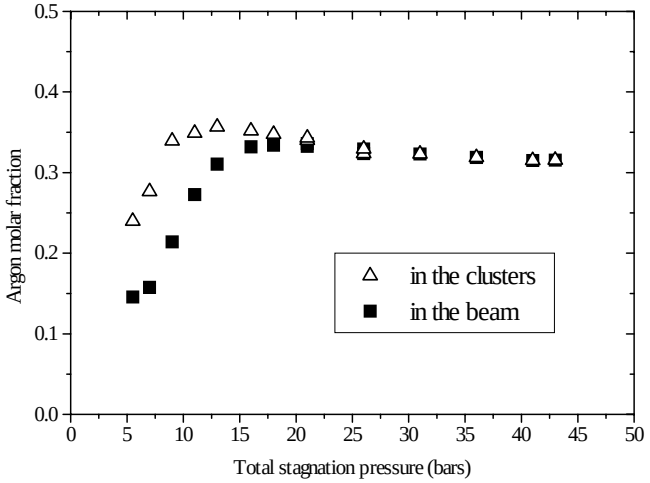

Fig. 5. Argon mf evolution with stagnation pressure for a 0.91 mf nitrogen—0.09 mf argon mixture in the beam and in the clusters.

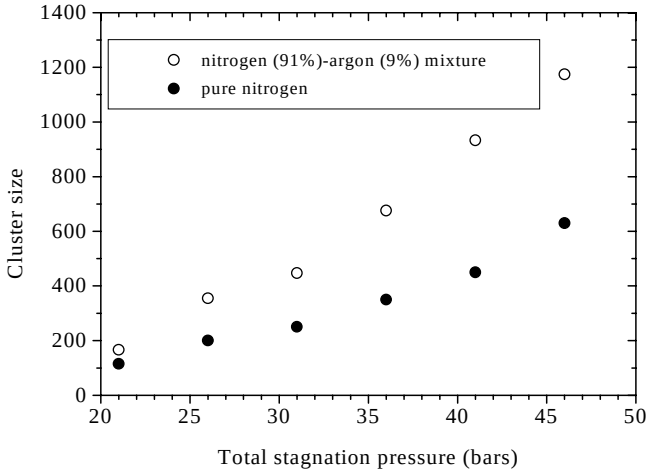

Fig. 6. Evolution with stagnation pressure of the average cluster sizes for a 0.91 mf nitrogen—0.09 mf argon mixture and a pure nitrogen beam.

more easily than nitrogen because of the focusing effect. As the stagnation pressure increases, the clusters enrich in argon. This is probably due to a combination of the greater ability for argon to nucleate over nitrogen and the Mach-number focusing effect which focuses the clusters rich in argon.

If we use these molar fraction measurements to define a beam weighted partial pressure for argon and nitrogen as the product of total stagnation pressure by the mf measured in the beam, we obtain the Figure 4b. It shows that the curves of the argon monomer percentage for the pure gas and for the mixture do coincide and that argon does significantly favor the nitrogen condensation. This gives a solution to the previous intriguing issue. Note that the gamma effect is not important since the vibration of the nitrogen molecule is negligible for the considered stagnation temperature.

As it was pointed out before, the results on the composition of mixed clusters (given by Fig. 5) are necessary for our size determination technique which needs an average molecular mass for the mixed clusters. Moreover, Figure 1c proves that the percentage of argon monomers inside the mixed condensed beam for a stagnation pressure higher than 21 bars is low. Hence, according to calculations [11], it is possible to use the buffer gas scattering technique down to about this pressure as long as we work with argon or mixed dimer profiles. This is satisfied with good approximation in the present case.

Figure 6 shows the obtained sizes. Comparison with pure nitrogen results confirm that the argon presence favors nucleation. Clusters formed by a pure argon gas expansion would be much larger for the same stagnation pressure (average size of 4400 atoms for 26 bars). The average cluster sizes obtained for the mixture lie between the sizes obtained for the pure gases.

4 Conclusion

The two complementary scattering techniques provide a simple and efficient way to obtain a series of results for mixed beam diagnostics. From the buffer gas scattering technique, one obtains both evidence for mixed cluster presence and their size. From the surface scattering technique, one deduces the percentage of uncondensed matter for the species in the beam and thus, the cluster composition.

Applying these techniques to a 0.91 mf nitrogen—0.09 mf argon mixture, we have proved the existence of mixed clusters and gathered significant results for a better understanding of the nucleation process. Nitrogen seems to help argon nucleation only because of the Mach-number focusing effect, but the resulting nucleation enhancement seems to be quite negligible. On the contrary, argon acting like seeds favors nitrogen condensation considerably.

The authors gratefully acknowledge M.-F. de Feraudy, Y. Loreaux and G. Torchet for fruitful discussions.

References

1. G. Torchet, M.-F. de Feraudy, B. Raoult, Z. Phys. **D 103**, 3074 (1995).
2. D. Frantz, J. Chem. Phys. **105**, 10030 (1996).
3. T. Gough, D. Knight, G. Scoles, Chem. Phys. Lett. **97**, 155 (1983).
4. M. Lengen, M. Joppien, R. von Pietrowski, T. Möller, Chem. Phys. Lett. **229**, 362 (1994).
5. A. Krylov, R. Gerber, M. Gaveau, J.-M. Mestdagh, B. Schilling, J.-P. Visticot, J. Chem. Phys. **104**, 3651 (1996).
6. J. Jortner, U. Even, A. Goldberg, I. Schek, T. Raz, R. Levine, Surf. Rev. Lett. **3**, 263 (1996).
7. V. Vorsa, S. Nandi, P. Campagnola, M. Larsson, W. Lineberger, J. Chem. Phys. **106**, 1402 (1997).

8. H. Haberland, *Clusters of Atoms and Molecules I.*, edited by H. Haberland, 2nd edn. (New York London Sydney: Springer 1995).
9. M. Châtelet, A. De Martino, J. Pettersson, F. Pradère, H. Vach, Chem. Phys. Lett. **196**, 563 (1992).
10. F. Pradère, M. Benslimane, M. Chateau, M. Bierry, M. Châtelet, D. Clement, A. Guilbaud, J.-C. Jeannot, A. De Martino, H. Vach, Rev. Sc. Instr. **65**, 161 (1994).
11. A. De Martino, M. Benslimane, M. Châtelet, C. Crozes, F. Pradère, H. Vach, Z. Phys. **D 27**, 185 (1993).
12. F. Pradère, M. Benslimane, M. Châtelet, A. De Martino, H. Vach, Surf. Sc. Lett. **375**, L375 (1997).
13. H. Vach, A. De Martino, M. Benslimane, M. Châtelet, F. Pradère, J. Chem. Phys. **100**, 3526 (1994).
14. H. Vach, M. Benslimane, M. Châtelet, A. De Martino, F. Pradère, J. Chem. Phys. **103**, 1972 (1995).
15. M. Benslimane, M. Châtelet, A. De Martino, F. Pradère, H. Vach, Chem. Phys. Lett. **237**, 223 (1995).
16. M. Benslimane, Ph.D. Thesis, Ecole Polytechnique 1995.
17. J. Hirschfelder, C. Curtiss, R. Byron Bird, Molecular Theory of Gases and Liquids (J. Wiley and Sons Inc., 1967).
18. L. Beneventi, P. Casavecchia, G. Volpi, C. Wong, F. McCourt, J. Chem. Phys. **98**, 7926 (1993).
19. O. Hagena, W. Obert, J. Chem. Phys. **56**, 1793 (1972).
20. M. Yamashita, T. Sano, S. Kotake, J. Fenn, J. Chem. Phys. **75**, 5355 (1981).
21. P. Sharma, E. Knuth, W. Young, J. Chem. Phys. **64**, 4345 (1976).